

# An Adaptive Transmitting Power Technique for Energy Efficient mm-Wave Wireless NoCs

Andrea Mineo  
University of Catania, Italy  
amineo@dieei.unict.it

Maurizio Palesi  
Kore University, Italy  
maurizio.palesi@unikore.it

Giuseppe Ascia  
and Vincenzo Catania  
University of Catania, Italy  
{gascia,vcatania}@dieei.unict.it

**Abstract**—Several emerging techniques have been recently proposed for alleviating the communication latency and the energy consumption issues in multi/many-core architectures. One of such emerging communication techniques, namely, WiNoC replaces the traditional wired links with the use of wireless medium. Unfortunately, the energy consumed by the RF transceiver (*i.e.*, the main building block of a WiNoC), and in particular by its transmitter, accounts for a significant fraction of the overall communication energy. In this paper we propose a runtime tunable transmitting power technique for improving the energy efficiency of the transceiver in wireless NoC architectures. The basic idea is tuning the transmitting power based on the location of the recipient of the current communication. The integration of the proposed technique into two known WiNoC architectures, namely, iWise64 and McWiNoC resulted in an energy reduction of 43% and 60%, respectively.

## I. INTRODUCTION

In the last few years, we are assisting to the transition from single-core to multi-core implementations and we are now entered in the so called many-core era. A number of chip makers, including Intel, AMD, TILER, *etc.*, have already released commercial multi/many-core products. For instance, AMD has recently released the first native eight core processor for the desktop market [1], while TILER and Intel have released a 72-core and a 60-core coprocessors, respectively [2], [3]. On the research side, Intel integrated 80 programmable cores into a single chip [4], and more recently, 45 P54C Pentium cores in a single chip, named SCC [5], which uses a Network-on-Chip (NoC) as interconnection fabric.

As the number of cores integrated into the same chip increases, the role played by the on-chip communication system becomes more and more important. The cost (*i.e.*, silicon area), the performance (*e.g.*, communication delay, throughput, *etc.*), and the energy consumption of the NoC are common design optimization metrics. For instance, with regards to the communication performance, as the network size increases, due to the multi-hop communication nature of NoC-based systems, the communication latency increases. To face with this problem, several emerging communication architectures have been proposed. Wireless NoCs (WiNoC) [6] use a wireless backbone upon the traditional wire-based NoC [7]. A WiNoC introduces new hardware structures such as antenna and transceivers, that represent an overhead in terms of area and power. The use of concentrated architectures and hierarchical topologies [8] is a viable solution to deal with the antenna area overhead issue. With regard to the power issue, the major contribution is due to the radio transmitter front-end connected to the antenna. For instance, in [9] the transmitter

is responsible for about 65% of the overall transceiver power consumption, while in [10] this contribution is more than 74%. Previous work in the context of WiNoCs consider transmitters in which the transmitting power is constant (regardless the distance of the destination node), and able to guarantee a given reliability level (in terms of bit error rate, BER) in the worst case.

In this paper we propose a novel mechanism for improving the energy efficiency of the transmitters in WiNoC architectures. The basic idea is allowing the transmitter to run-time select its transmitting power based on the reliability requirements and the destination node of the current communication. We provide a systematic approach that, under a reliability constraint (given in terms of maximum BER) and for each antenna, allows to determine the optimal transmitting power for each destination node. The optimal transmitting power is off-line computed by using an accurate 3D field solver for a limited number of measurements. The obtained power figures are then used for configuring the proposed variable gain controller which is responsible of driving the power amplifier connected to the transmitting antenna. We found that, by integrating the proposed technique into two known WiNoC architectures, namely, iWise64 [8] and McWiNoC [11], results in an energy reduction of 48% and 50%, respectively. As compared to a traditional wire-line NoC, the energy saving of the augmented iWise64 and McWiNoC is 65% and 61%, respectively.

The rest of the paper is organized as follows. Section II reviews related works in the context of wireless NoCs. Section III provides a background on how estimating the signal attenuation in the wireless medium and the power strength requirements for the ASK-OOK modulation. The proposed technique along with the implementation details is presented in Section IV. Experimental results are presented in Section V. Finally, Section VI, concludes the paper and outlines the directions for future developments.

## II. RELATED WORK

The capability of integrating an antenna with its transceiver onto a silicon die [12] has lead several research groups to assess the advantages of having long range wireless links upon the traditional wire-based NoCs. An exhaustive panoramic of the state-of-the-art in WiNoC architectures can be found in [7]. Here, the authors divide the various WiNoC architectures into two main classes, namely, mesh based topology and small-world based topology WiNoCs. Another classification can be done on the basis of the portion of electromagnetic

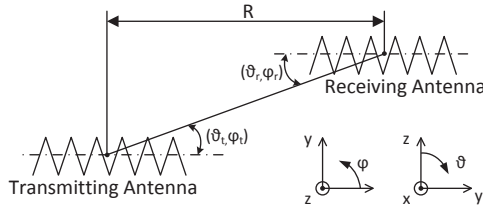


Fig. 1. Friis transmission equation: geometrical orientation of transmitting and receiving antennas. As indicated, considering a spherical coordinate system,  $\phi$  is the azimuthal angle in the XY plane, where the X axis is  $0^\circ$  and Y axis is  $90^\circ$ .  $\theta$  is the elevation angle where the Z-axis is  $0^\circ$ , and the XY plane is  $90^\circ$ .

spectrum used for data transmission such as UWB [6] (few GHz), mm-wave [8], [13]–[15] (tens of GHz), sub-THz [16] (hundreds of GHz), and THz [17] NoC. While the first three use the metallization present in standard CMOS technology as antenna, the latter makes use of carbon nanotubes.

In mm-wave WiNoCs, zigzag antenna is viewed as the best candidate solution for on-chip antenna [7]. In this paper we consider zigzag antenna as its behavior can be more easily predicted with already consolidated techniques and knowledge such as the use of field solvers for modeling and analysis. Furthermore, the use of regular topologies, like 2D meshes, allows the exploitation of symmetries that simplify their characterization. Several examples of mesh based WiNoC architectures can be found in literature [8], [11], [16], [18]. For adapting the baseband signal to the wireless medium, in this context, the most used modulation is Amplitude Shift Keying or On Off Keying (ASK-OOK) [7], [8], [13]. Although, for a given BER, the ASK-OOK modulation requires a higher transmitting power than that required by other kinds of modulation (e.g., the Quadrature Amplitude Modulation (QAM) [19]), and has a poor spectral efficiency, its hardware implementation is simple (low area overhead as compared to QAM) and tailored to be applied in the on-chip context. In this paper, we propose a technique and circuitry for improving the power efficiency of a ASK-OOK transceiver by means of a reliability aware on-line transmitting power modulation.

### III. BACKGROUND

This section provides a brief background on the Friis transmission equation used for computing the fraction of transmitting power that reaches the receiving antenna. Consequently, it introduces the formula used for computing the minimum transmitting power to guarantee a certain BER.

#### A. Friis Transmission Equation

The required transmitting power depends on many factors, including, the kind of modulation, the transceiver noise figure, and the attenuation introduced by the wireless medium. Let us consider the Fig. 1 which shows a transmitting antenna with an output power  $P_t$  and a relative angle respect the receiving antenna of  $(\theta_t, \phi_t)$ , and a receiving antenna, located at distance  $R$ , with a relative angle respect the transmitting antenna of  $(\theta_r, \phi_r)$ . The fraction of the transmitting power that reaches the terminal of the receiving antenna,  $P_r$ , can be computed with the well known Friis transmission equation [20] valid when  $R > 2D^2/\lambda$ , where  $D$  is the the maximum dimension of antenna (axial length in our case) and  $\lambda$  is the wavelength.

The Friis equation is:

$$G_a = \frac{P_r}{P_t} = e_t e_r \frac{\lambda^2 D_t(\theta_t, \phi_t) D_e(\theta_r, \phi_r)}{(4\pi R)^2} \cdot (1 - |\Gamma_t|)(1 - |\Gamma_r|) |\hat{\rho}_t \cdot \hat{\rho}_r| \quad (1)$$

where:

- $e_t$  and  $e_r$  are the efficiencies of the transmitting and receiving antenna, respectively. These parameters mainly represent the signal losses in the silicon substrate. For reducing such contribution, high resistivity Silicon on Insulator (SoI) substrates ( $> 1 \text{ K}\Omega\text{cm}$ ) can be used [21] or a polyamide stratus (few micron thick) can be inserted under the antenna [16].
- $D_t$  and  $D_r$  are the directivities of the transmitting and receiving antenna, respectively. They quantify how much better the antenna can transmit or receive in a specific direction.
- $\lambda$  is the effective wavelength. For an IC substrate, it is estimated by using the material properties of the top IC layers (silicon dioxide  $\epsilon_r = 3.9$ ) [22].
- $|\Gamma|$  refers to the portion of the transmitting/receiving power that returns to the transceiver due to impedance mismatch (ideally  $|\Gamma| = 0$ ). This parameter is known as reflection coefficient.
- $|\hat{\rho}_t \cdot \hat{\rho}_r|$  takes into account the polarization status of the emitted EM wave (ideally, it is equal to one).

Eqn. (1) highlights the parameters which determine the gain  $G_a$ . However, in practical cases,  $G_a$  computation is performed by means of Eqn. (2).

$$G_a = \frac{P_r}{P_t} = \frac{|S_{12}|}{(1 - |S_{11}|)(1 - |S_{22}|)} \quad (2)$$

where,  $S_{11}$ ,  $S_{12}$ , and  $S_{22}$  are the scattering parameters. Such parameters are computed by using field solver simulation tools [23] or by direct measures from realized prototypes.

#### B. Signal Strength Requirements

Using Eqn. (2) we can estimate the signal attenuation due to the wireless medium. Since the reliability of the ASK-OOK modulation is related to the energy per bit,  $E_b$ , spent to reach the receiver's antenna, we can determine the power required by the transmitter for each value of attenuation  $G_a$ . In particular, for the ASK-OOK modulation the bit error rate can be computed as:

$$BER = Q\left(\sqrt{\frac{E_b}{N_0}}\right) \quad (3)$$

where  $N_0$  is the transceiver noise spectral density and the  $Q$  function is the tail probability of the standard normal distribution. Since  $E_b = P_r/R_b$ , where  $P_r$  is the power received at the terminal of the receiver antenna while  $R_b$  is the data rate, we can compute the required transmitting power for a given data rate and BER requirement and for a given transceiver's thermal noise as:

$$P_r = E_b \cdot R_b = [Q^{-1}(BER)]^2 2N_0R_b \quad (4)$$

where  $Q^{-1}$  is the inverse of the  $Q$  function.

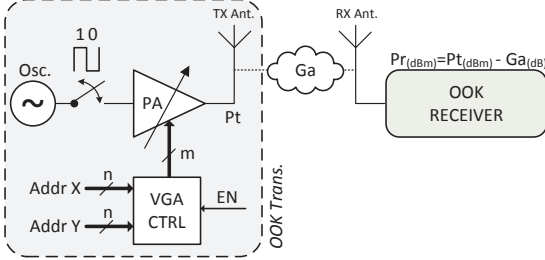


Fig. 2. Transceiver scheme.

Thus, the minimum transmitting power to reach a certain receiver guaranteeing a maximum BER can be computed as:

$$P_t(\text{dBm}) = P_r(\text{dBm}) - G_a(\text{dB}) \quad (5)$$

where  $P_r(\text{dBm})$  is given by Eqn. (4) while  $G_a(\text{dB})$  is computed by using a field solver with the Friis formula when power is expressed in dBm.<sup>1</sup>

#### IV. ADAPTIVE TRANSMITTING POWER TRANSCEIVER

This section presents a variable gain controller, used to drive the power amplifier in the RF transceiver, which adaptively determines the optimal transmitting power for the current communication. In addition, the section provides the basic steps to be performed for configuring the controller.

##### A. Variable Gain Controller

As discussed in the introduction and in the related work sections, traditional transceivers in WiNoCs use the same transmitting power regardless to the distance (location) of the destination node. In fact, the transmitting power is set for the worst case under a reliability (*i.e.*, maximum BER) constraint. We propose of runtime tuning the transmitting power based on the physical location of the destination node of the current communication by ensuring a maximum BER.

Given a maximum admissible BER, the designer must choose the minimal transmitting power which allows the communication between the radio hubs. The selection of the transmitting power to be used for all the communications impacts the energy consumption of the power amplifier (PA). It also determine the attenuation level of the inter-channel interference when communications use different frequencies (FDM). Based on this, we augmented the transceiver with a novel capability, namely, adaptive transmitting power tuning. That is, instead of using the worst case transmitting power regardless to the destination, we propose of runtime tuning the transmitting power based on the recipient of the current communication. This is accomplished by the use of a PA in which the output power can be configured online as in [10]. It is already an established technique in the context of radio communications (*e.g.*, mobile phones, wireless sensors network, *etc.*), but it requires sophisticated controller policies. Fortunately, in the context of on-chip wireless communication, thanks to the regularity of the 2D mesh topology, we can define a simple scheme for runtime tuning the transmitting power.

Fig. 2 shows the proposed transceiver in which the transmitting power is controlled by a specific block called variable gain amplifier (VGA) controller. The output of the VGA controller

drives the power amplifier controllable circuitry. The VGA controller uses the destination address stored in the head flit of the packet for determining the optimal transmitting power level. The optimal transmitting power level for each destination is computed offline and stored into a lookup table in the VGA controller as it will be described in the next subsection.

##### B. Determining the Transmitting Power Map

Let us now provide the basic steps needed for determining the optimal transmitting power for each node pairs assuming a 2D mesh topology. Such transmitting power information are clustered with a certain granularity based on the number of power steps used by the PA and stored into a lookup table in the VGA controller. The basic steps are summarized as follows.

- 1) Compute the attenuation map. For each pair <transmitting antenna, receiving antenna>, extract the scattering parameters  $S_{11}$  and  $S_{22}$  and compute the gain by means of Eqn. (2). In case of the availability of a test-chip, the scattering parameters  $S_{11}$  and  $S_{22}$  can be directly measured by means of a network analyzer [24].
- 2) Compute the Power map. For each pair <transmitting antenna, receiving antenna>, based on the required transmission data rate and the maximum allowed BER, apply Eqn. (4) and then Eqn. (5) for computing the optimal transmitting power.
- 3) Configure the VGA controller. Upload the lookup table in each VGA controller with the information computed at the previous step. The lookup table has a number of entries equal to the number of destinations (*i.e.*, receiving antennas). Each entry contains the power step code used to drive the PA. Of course, for a required transmitting power  $P$ , the selected power step is such that the transmitting power  $P_t$  is greater-equal than  $P$ .

In the following section we will assess the effectiveness of the proposed technique in communication energy consumption reduction.

#### V. EXPERIMENTS

In this section we present the results of experiments considering a mesh-based WiNoC on a  $20\text{mm} \times 20\text{mm}$  silicon die. A zigzag antenna has been accurately modeled and characterized with Ansoft HFSS [25] (High Frequency Structural Simulator). HFSS is a leading commercial finite element method (FEM) field solver which simulates 3D structures and produces S-parameters and radiation patterns. We considered an high resistivity  $\rho = 5 \text{ K}\Omega\text{cm}$  SOI with a substrate thickness of  $350 \mu\text{m}$  and  $30 \mu\text{m}$  for the oxide ( $\text{SiO}_2$ ). The antennas are situated at an elevation of  $2 \mu\text{m}$  from the substrate, compatibly with the guidelines reported in [26] for reducing the interference with others metal structures ([26] demonstrates that the interference due to other metallic structures is negligible by following such rules). The zigzag antenna has a thickness of  $2 \mu\text{m}$  and an axial length of  $2 \times 340 \mu\text{m}$  for operating at around 60 GHz. The same setup has been used in [21].

From HFSS simulation we obtain the scattering parameters ( $S_{11}$  and  $S_{12}$ ) used for computing the Friis formula and then for calculating the attenuation introduced by the wireless medium. In particular,  $S_{11}$  is also used for determining the antenna bandwidth as discussed in the following subsection.

<sup>1</sup>The absolute power,  $P$ , can be expressed in dBm by  $P_{\text{dBm}} = 10 \cdot \log(P \cdot 10^3)$

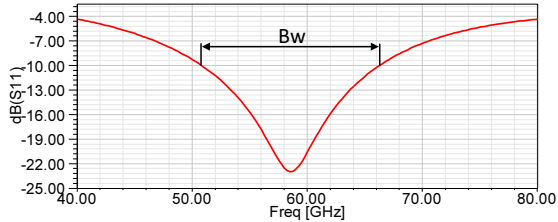


Fig. 3.  $S_{11}$  parameter of the zigzag antenna. The bandwidth is the range of frequency under -10 dB.

#### A. Bandwidth and Radiation Pattern

Fig. 3 shows the  $S_{11}$  parameter which quantifies the portion of transmitting power that comes back to the power amplifier due to impedance mismatch ( $50 \Omega$ ). Based on a thumb rule [20], we can assume that the antenna matches with the transceiver when, at the operating frequency, the  $S_{11}$  is less than -10 dB. We used  $S_{11}$  for defining the antenna bandwidth because out of the range of frequencies for which  $S_{11} < -10$  dB, the antenna not only does not work properly as transducer but it could affect the physical integrity of the final stage of the PA.

Thus, looking at Fig. 3, a bandwidth of about 16 GHz is enough for providing a data rate upper bound of 16 Gbps with ASK-OOK modulation. Let us indicate with  $B_W$  such bandwidth, the antenna relative bandwidth is:

$$B_r = \frac{B_W}{f_c} = \frac{16 \text{ GHz}}{59 \text{ GHz}} = 0.27$$

where  $f_c$  is the resonance frequency. Such information is useful for determining at which resonance frequency we should design the antenna for obtaining data rates higher than 16 Gbps, or if we are interested in having more bandwidth for a frequency division multiplexing (FDM). For instance, for 4 channels with a data rate of 16 Gbps, we can design an antenna with a resonance frequency of at least:

$$f_c = \frac{B_W}{B_r} = \frac{4 \times 16 \text{ GHz}}{0.27} = 237 \text{ GHz}$$

which is obtainable by properly scaling the dimensions of the antenna (mainly the axial length).

Another important result from simulation is the normalized radiation pattern shown in Fig. 4. The radiation pattern is a polar representation of the directivity represented by the term  $D$  in Eqn. (1). As it can be observed, the best performance is obtained when the antenna transmits or receives in the direction of its main axis. With this information we can have an idea of the attenuation in a particular direction Eqn. (1) as it will be shown in the experimental section.

#### B. Attenuation Maps

Let us consider a mesh based WiNoC formed by a set of  $T$  tiles and a radio hub for each tile. Let us now analyze the attenuation of the signal transmitted by an antenna in a tile  $t \in T$  as viewed by the remaining antennas located at tiles  $T \setminus \{t\}$ . In the experiments we considered  $|T| = 16$  in which the distance between two antennas in the same axis is 2.5 mm.

Fig. 5 shows the attenuation  $G_a$  for a transmitting antenna located on tile  $t_0$ ,  $t_1$ ,  $t_4$ , and  $t_5$ . The other attenuation maps (*i.e.*, the attenuations when the transmitting antenna is located

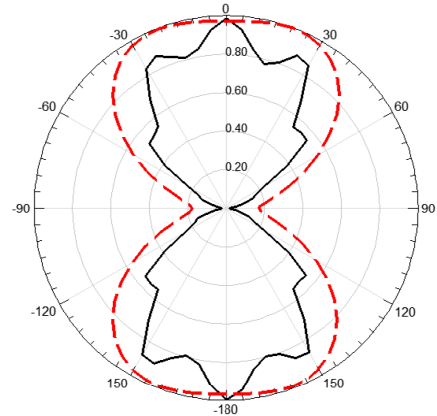


Fig. 4. Radiation pattern for a zigzag antenna at the horizon ( $\phi = 90^\circ$ , continuous line) and at the elevation of maximum radiation ( $\phi = 35^\circ$ , dashed line).  $\theta = 0^\circ$  is the direction parallel to the antenna's main axis while  $\theta = 90^\circ$  is the orthogonal direction. According to Fig. 1, we assume the antenna situated upon the XY plane.

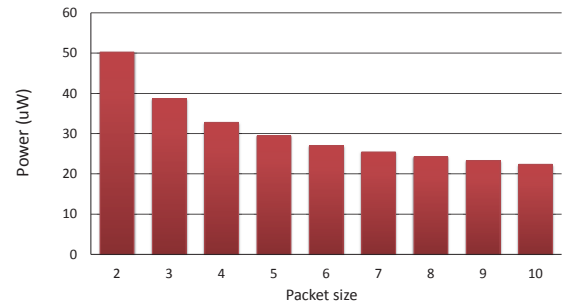


Fig. 6. Power analysis of VGA controller: varying the packet length, the toggle rate of his internal node is reduced.

in other tiles) can be found by symmetry. In fact, the antenna exhibits very different behavior when it is placed in different locations within the die [22]. Thus, the measures should be performed by considering all the possible positions for the transmitting and receiving antenna. Fortunately, due to the symmetrical structure of mesh-based topologies, only four measurements are needed in our case. For instance, the attenuation observed by a receiving antenna at tile  $t_{13}$  when the transmitting antenna is on tile  $t_{12}$ ,  $G_a(t_{12}, t_{13})$ , is the same observed by the receiving antenna located on tile  $t_1$  when the transmitting antenna is on tile  $t_0$ ,  $G_a(t_0, t_1)$ . Similarly, we have  $G_a(t_{15}, t_{14}) = G_a(t_0, t_1)$ ,  $G_a(t_3, t_2) = G_a(t_0, t_1)$ , and so on. In addition,  $G_a(t_x, t_y) = G_a(t_y, t_x)$  for each  $t_x, t_y \in T$ .

As can be observed from Fig. 5, the attenuation introduced by the wireless medium does not depend only on the relative distance between the radio hubs but it depends also on their relative orientation. For instance,  $G_a(t_0, t_3) < G_a(t_0, t_4)$  although the distance between  $t_0$  and  $t_3$  is three times higher than the distance between  $t_0$  and  $t_4$ . This can be explained observing the radiation pattern in Fig. 4 in which the performance of the antenna increases as it transmits to or receives from its main axis direction.

#### C. Energy Saving

Let us now compute the maximum and minimum transmitting power for guaranteeing a certain reliability level. For the sake of example, let us consider a maximum BER of  $3 \times 10^{-14}$

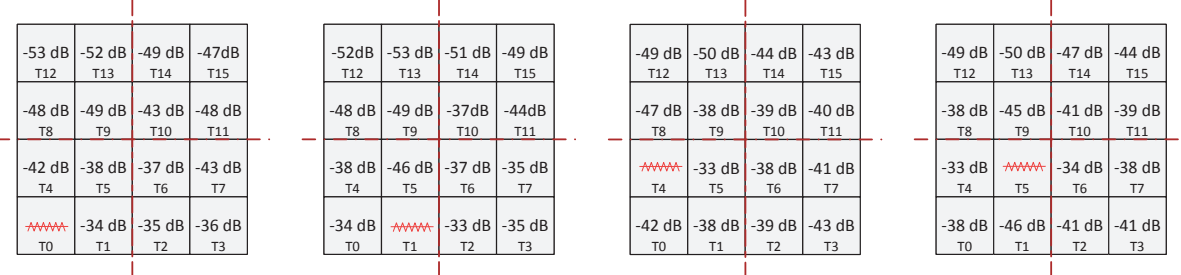


Fig. 5. HFSS Simulation results: attenuation map ( $G_a$ ) for the tiles  $t_0, t_1, t_4$  and  $t_5$ . The others map can be obtained considering the structure's symmetries.

and a data rate of 16 Gbps. From Eqn. (4) we have that the power received by the receiving antenna must be  $-54$  dBm. From the attenuation maps shown in Fig. 5, the maximum attenuation is  $-53$  dBm. Thus, the transmitting power (which is maximum as this is the worst case) is computed by Eqn. (5) as  $P_{t,max} = -54 - (-53) = -1$  dBm, that in linear scale is  $P_{t,max} = 794 \mu\text{W}$ . Similarly we can compute the minimal transmitting power. The minimum attenuation is  $-33$  dBm, thus  $P_{t,min} = -54 - (-33) = -21$  dBm, that in linear scale is  $P_{t,min} = 8 \mu\text{W}$ .

Now, let us consider the transceiver proposed in [10], also used in [8], which has 7 adjustable output power steps. We described the VGA controller in RTL using Synopsys Design Compiler and applied the proposed scheme to two specific architectures, namely, McWiNoC [11] and iWise [8]. For the transceiver we estimate a power consumption of 7 mW to 23 mW for the minimum and maximum transmitting power, respectively. They corresponding to an energy per bit ranging from 0.42 pJ/bit to 1.4 pJ/bit.

The power figures for the VGA controller with a control output of 3 bits (7 power steps), have been estimated with Synopsys Power Compiler for different packet sizes. In fact, as packet size increases, the toggle rate of the VGA controller decreases as it is active only for the head flit of the packet. Fig. 6 shows the average power dissipation of the VGA controller for different packet size considering a 28 nm CMOS standard cell library from TSMC operating at 1 GHz. As it can be observed, for a 10-flit packet, the average power dissipation of the VGA controller is as low as  $21 \mu\text{W}$  which is negligible as compared to the power dissipated by the other elements of the transceiver and the router, both in the order of milliwatt. With regard to the overhead in terms of silicon area and timing, the area of the VGA controller is  $80 \mu\text{m}^2$  (about four order of magnitude less than a traditional transceiver) and its delay is about 8 FO4.

Power data have been used for back-annotating a cycle accurate NoC simulator based on Noxim [27] and augmented with wireless communication. The following NoC architectures have been compared in terms of energy.

- 1) Wire-line:  $8 \times 8$  concentrated mesh, with clusters of 4 cores.
- 2) McWiNoC: The architecture described in [11] for a  $8 \times 8$  mesh with 4 cores associated with each radio hub. This kind of architecture uses TDM multiplexing for the wireless medium. The entire 16 Gbps of bandwidth can be allocated for each communications due to the particular structure of the architecture.
- 3) Proposed McWiNoC: Like McWiNoC but augmented

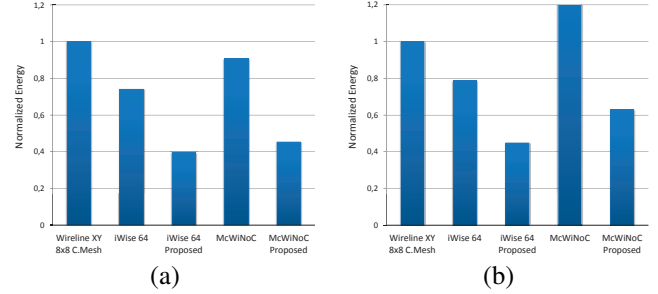


Fig. 7. Normalized energy consumption under uniform traffic (a) and for a real case study (b).

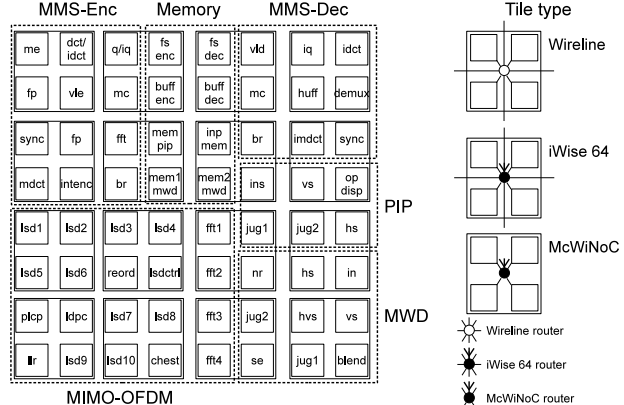


Fig. 8. Heterogeneous system composed by a multimedia sub-system, a MIMO-OFDM receiver, a PIP and a MWD module.

with the proposed VGA controller.

- 4) iWise64: The architecture described in [8] in which there are 4 channels with 4 Gbps of bandwidth.
- 5) Proposed iWise64: Like iWise64 but augmented with the proposed VGA controller.

Fig. 7(a) shows the normalized energy (assuming the wire-line NoC as baseline) of the different architectures under uniform traffic. As can be observed, up to 48% and 50% of energy saving is obtained by using the proposed VGA controller in iWise64 and McWiNoC, respectively. As compared to the baseline wire-line NoC, up to 61% and 65% of energy saving is obtained.

Finally, as a real case study, we consider a complex heterogeneous system shown in Fig. 8. The system is composed by a generic MultiMedia System which includes a H.263 video encoder, a H.264 video decoder, a MP3 audio encoder and

a MP3 audio decoder [28], a MIMO-OFDM receiver [29], a Picture-In-Picture application (PiP) [30] and a Multi-Window Display application (MWD) [31]. The normalized energy savings are shown in Fig. 7(b). Once again, the application of the proposed technique results in interesting energy saving up to 60% and 43% when applied to McWiNoC and iWise64, respectively.

## VI. CONCLUSIONS

Emerging communication technologies like wireless NoC (WiNoC) are considered as a viable solution for facing the scalability and the energy consumption issues in many-core system architectures. Unfortunately, the transceiver of the radio hub in a WiNoC accounts for a significant fraction of the overall communication energy budget. In this paper we have presented a reliability aware runtime tunable transmitting power technique for improving the energy efficiency of the transceiver in wireless NoC architectures. We have applied the proposed technique to two known WiNoC architectures, namely, iWise64 [8] and McWiNoC [11] observing an energy reduction up to 43% and 60%, respectively. The hardware overhead, in terms of silicon area, due to implement the proposed technique is negligible as compared to the area of the transceiver (about four order of magnitude less than the transceiver).

We believe that the introduction of the proposed technique opens interesting scenarios in several directions. For instance, application mapping strategies might take into account the specific radiation patterns of the antenna or design space exploration techniques might consider the orientation of the antennas as an additional degree of freedom for application specific optimization purposes.

## REFERENCES

- [1] AMD. FX 8-core processor. [Online]. Available: <http://www.amd.com/>
- [2] Tilera. TILE-Gx8072 processor. [Online]. Available: <http://www.tilera.com/>
- [3] R. Courtland, "What intels xeon phi coprocessor means for the future of supercomputing," *IEEE Spectrum*, 2013.
- [4] S. R. Vangal, J. Howard, G. Ruhl, S. Dighe, H. Wilson, J. Tschanz, D. Finan, A. Singh, T. Jacob, S. Jain, V. Erraguntla, C. Roberts, Y. Hoskote, N. Borkar, and S. Borkar, "An 80-tile sub-100-W TeraFLOPS processor in 65-nm CMOS," *IEEE Journal of Solid-State Circuits*, vol. 43, no. 1, pp. 29–41, Jan. 2008.
- [5] A.-M. Corley. (2010, Feb.) Intel lifts the hood on its single-chip cloud computer. [Online]. Available: <http://spectrum.ieee.org/>
- [6] D. Zhao and Y. Wang, "Sd-mac: Design and synthesis of a hardware-efficient collision-free qos-aware mac protocol for wireless network-on-chip," *Computers, IEEE Transactions on*, vol. 57, no. 9, pp. 1230–1245, 2008.
- [7] S. Deb, A. Ganguly, P. Pande, B. Belzer, and D. Heo, "Wireless noc as interconnection backbone for multicore chips: Promises and challenges," *Emerging and Selected Topics in Circuits and Systems, IEEE Journal on*, vol. 2, no. 2, pp. 228–239, 2012.
- [8] D. DiTomaso, A. Kodi, S. Kaya, and D. Matolak, "iwise: Inter-router wireless scalable express channels for network-on-chips (nocs) architecture," in *High Performance Interconnects (HOTI), 2011 IEEE 19th Annual Symposium on*, 2011, pp. 11–18.
- [9] X. Yu, S. Sah, S. Deb, P. Pande, B. Belzer, and D. Heo, "A wideband body-enabled millimeter-wave transceiver for wireless network-on-chip," in *Circuits and Systems (MWSCAS), 2011 IEEE 54th International Midwest Symposium on*, 2011, pp. 1–4.
- [10] D. Daly and A. Chandrakasan, "An energy-efficient ook transceiver for wireless sensor networks," *Solid-State Circuits, IEEE Journal of*, vol. 42, no. 5, pp. 1003–1011, 2007.
- [11] D. Zhao, Y. Wang, J. Li, and T. Kikkawa, "Design of multi-channel wireless noc to improve on-chip communication capacity!" in *Networks on Chip (NoCS), 2011 Fifth IEEE/ACM International Symposium on*, 2011, pp. 177–184.
- [12] J. Lin, H.-T. Wu, Y. Su, L. Gao, A. Sugavanam, J. Brewer, and K. O, "Communication using antennas fabricated in silicon integrated circuits," *Solid-State Circuits, IEEE Journal of*, vol. 42, no. 8, pp. 1678–1687, 2007.
- [13] S. Deb, A. Ganguly, K. Chang, P. Pande, B. Beizer, and D. Heo, "Enhancing performance of network-on-chip architectures with millimeter-wave wireless interconnects," in *Application-specific Systems Architectures and Processors (ASAP), 2010 21st IEEE International Conference on*, 2010, pp. 73–80.
- [14] S. Deb, K. Chang, A. Ganguly, X. Yu, C. Teuscher, P. Pande, D. Heo, and B. Belzer, "Design of an efficient noc architecture using millimeter-wave wireless links," in *Quality Electronic Design (ISQED), 2012 13th International Symposium on*, 2012, pp. 165–172.
- [15] S. Deb, K. Chang, M. Cosic, A. Ganguly, P. P. Pande, D. Heo, and B. Belzer, "CMOS compatible many-core noc architectures with multi-channel millimeter-wave wireless links," in *Proceedings of the great lakes symposium on VLSI*, ser. GLSVLSI '12. New York, NY, USA: ACM, 2012, pp. 165–170.
- [16] S.-B. Lee, S.-W. Tam, I. Pefkianakis, S. Lu, M. F. Chang, C. Guo, G. Reinman, C. Peng, M. Naik, L. Zhang, and J. Cong, "A scalable micro wireless interconnect structure for CMPs," in *Proceedings of the 15th annual international conference on Mobile computing and networking*, ser. MobiCom '09. New York, NY, USA: ACM, 2009, pp. 217–228.
- [17] A. Ganguly, K. Chang, S. Deb, P. Pande, B. Belzer, and C. Teuscher, "Scalable hybrid wireless network-on-chip architectures for multicore systems," *Computers, IEEE Transactions on*, vol. 60, no. 10, pp. 1485–1502, 2011.
- [18] C. Wang, W.-H. Hu, and N. Bagherzadeh, "A wireless network-on-chip design for multicore platforms," in *Parallel, Distributed and Network-Based Processing (PDP), 2011 19th Euromicro International Conference on*, 2011, pp. 409–416.
- [19] L. Couch, *Digital and Analog Communication Systems*, ser. Pearson international edition. Pearson/Prentice Hall, 2007.
- [20] C. Balanis, *Modern Antenna Handbook*. Wiley, 2008.
- [21] S. Montusclat, F. Giancesello, D. Gloria, and S. Tedjini, "Silicon integrated antenna developments up to 80 ghz for millimeter wave wireless links," in *Wireless Technology, 2005. The European Conference on*, 2005, pp. 237–240.
- [22] F. Gutierrez, S. Agarwal, K. Parrish, and T. Rappaport, "On-chip integrated antenna structures in cmos for 60 ghz wpan systems," *Selected Areas in Communications, IEEE Journal on*, vol. 27, no. 8, pp. 1367–1378, 2009.
- [23] B. Floyd, C.-M. Hung, and K. O, "Intra-chip wireless interconnect for clock distribution implemented with integrated antennas, receivers, and transmitters," *Solid-State Circuits, IEEE Journal of*, vol. 37, no. 5, pp. 543–552, 2002.
- [24] K. O, K. Kim, B. Floyd, J. Mehta, H. Yoon, C.-M. Hung, D. Bravo, T. Dickson, X. Guo, R. Li, N. Trichy, J. Caserta, I. Bomstad, W.R., J. Branch, D.-J. Yang, J. Bohorquez, E. Seok, L. Gao, A. Sugavanam, J. J. Lin, J. Chen, and J. Brewer, "On-chip antennas in silicon ics and their application," *Electron Devices, IEEE Transactions on*, vol. 52, no. 7, pp. 1312–1323, 2005.
- [25] Ansoft HFSS. [Online]. Available: <http://www.ansys.com/>
- [26] E. Seok and K. Kenneth, "Design rules for improving predictability of on-chip antenna characteristics in the presence of other metal structures," in *Interconnect Technology Conference, 2005. Proceedings of the IEEE 2005 International*, 2005, pp. 120–122.
- [27] F. Fazzino, M. Palesi, and D. Patti, "Noxim: Network-on-Chip simulator," <http://noxim.sourceforge.net>.
- [28] J. Hu and R. Marculescu, "Energy- and performance-aware mapping for regular NoC architectures," *IEEE Transactions on Computer-Aided Design of Integrated Circuits and Systems*, vol. 24, no. 4, pp. 551–562, Apr. 2005.
- [29] S.-R. Yoon, J. Lee, and S.-C. Park, "Case study: Noc based next-generation wlan receiver design in transaction level," in *International Conference on Advanced Communication Technology*, 2006, pp. 1125–1128.
- [30] E. G. T. Jaspers and P. H. N. de With, "Chip-set for video display of multimedia information," *IEEE Transactions on Consumer Electronics*, vol. 45, no. 3, pp. 706–715, Aug. 1999.
- [31] E. B. van der Tol and E. G. Jaspers, "Mapping of MPEG-4 decoding on a flexible architecture platform," *Media Processors*, vol. 4674, pp. 362–375, 2002.